THE ASTROPHYSICAL JOURNAL, 458:621–636, 1996 February 20

ASSESSMENT OF THE POLYCYCLIC AROMATIC HYDROCARBON–DIFFUSE INTERSTELLAR BAND PROPOSAL

F. SALAMA,[1] E. L. O. BAKES,[2] L. J. ALLAMANDOLA,[1] AND A. G. G. M. TIELENS[1]
Received 1995 May 11; accepted 1995 August 25

ABSTRACT

The potential link between neutral and/or ionized polycyclic aromatic hydrocarbons (PAHs) and the diffuse interstellar band (DIB) carriers is examined. Based on the study of the general physical and chemical properties of PAHs, an assessment is made of their possible contribution to the DIB carriers. It is found that, under the conditions reigning in the diffuse interstellar medium, PAHs can be present in the form of neutral molecules as well as positive and/or negative ions. The charge distribution of small PAHs is dominated, however, by two charge states at one time with compact PAHs present only in the neutral and cationic forms. Each PAH has a distinct spectral signature depending on its charge state. Moreover, *the spectra of ionized PAHs are always clearly dominated by a single band in the DIB spectral range.* In the case of compact PAH ions, the strongest absorption band is of type A (i.e., the band is broad, falls in the high-energy range of the spectrum, and possesses a large oscillator strength), and seems to correlate with strong and broad DIBs. For noncompact PAH ions, the strongest absorption band is of type I (i.e., the band is narrow, falls in the low-energy range of the spectrum, and possesses a small oscillator strength), and seems to correlate with weak and narrow DIBs. Potential molecular size and structure constraints for interstellar PAHs are derived by comparing known DIB characteristics to the spectroscopic properties of PAHs. It is found that (i) only neutral PAHs larger than about 30 carbon atoms could, if present, contribute to the DIBs. (ii) For compact PAHs, only ions with less than about 250 carbon atoms could, if present, contribute to the DIBs. (iii) The observed distribution of the DIBs between strong/moderate and broad bands on the one hand and weak and narrow bands on the other can easily be interpreted in the context of the PAH proposal by a distribution of compact and noncompact PAH ions, respectively. A plausible correlation between PAH charge states and DIB "families" is thus provided by the PAH-DIB proposal. Following this proposal, DIB families would reflect conditions within a cloud which locally determine the relative importance of cations, anions, and neutral species, rather than tracers of a specific species. Observational predictions are given to establish the viability of the PAH hypothesis. It is concluded that small PAH ions are very promising candidates as DIB carriers provided their population is dominated by a finite number (100–200) of species. A key test for the PAH proposal, consisting of laboratory and astronomical investigations in the ultraviolet range, is called for.

Subject headings: dust, extinction – ISM: molecules — line: identification — molecular processes

1. INTRODUCTION

The diffuse interstellar bands (DIBs) are a number of weak absorption features superposed on the interstellar extinction curve. They fall in the visible and near-infrared spectral region, with the shortest and longest wavelengths known at 4177 and 13175 Å (Jenniskens & Désert 1994; Joblin et al. 1990). A weak band has been detected at 1369 Å quite recently in the spectrum of ζ Ophiuchi which may also be part of the DIB family (Tripp, Cardelli, & Savage 1994). Most of the estimated 100 (Herbig 1975, 1988, 1993; Herbig & Leka 1991)–200 (Jenniskens & Désert 1994) known bands fall between 4000 and 9000 Å. The individual DIBs vary widely in strength and shape, with equivalent width per magnitude of visual extinction ranging from about 2 Å to the detection limit of about 0.006 Å. The full width at half-maximum (FWHM) values for the DIBs range from about 0.6 to 40 Å. In general, the DIBs show a loose correlation with each other and with various interstellar dust and gas column density indicators, betraying their interstellar origin. However, in recent years, it has become increasingly clear that these correlations are not strict; i.e., maintained along all lines of sight. Indeed, while families of (strongly correlating) bands were recognized only a few years back (Krelowski & Walker 1987), it now almost seems as if the strength of any DIB can vary (to some extent) independently from all other DIBs (Krelowski & Sneden 1994). These variations are particularly clear when comparing lines of sight with well-defined physical conditions (i.e., those with single clouds; Krelowski & Sneden 1993), but become less obvious when averages over many clouds are considered. Due to this complexity, determining the correlation and relative strength of various DIBs is painstaking labor which is only now slowly bearing fruit. It must be stressed, however, that much of the conclusions drawn on the general behavior of the DIBs rely on the detailed study of only a few specific interstellar bands with a focus on the strongest ones (namely the 4430, 5780, 5797, 6284, and 6614 Å DIBs; Salama 1993; Somerville 1993). This is largely due, of course, to the difficulty of observing the weaker features and, hence, deriving reliable conclusions concerning their variation with other interstellar properties (interstellar tracers, reddening, etc.).

Several of the stronger DIBs—notably the 5780 and 6284 Å bands—have been detected toward some carbon-rich objects (Pritchet & Grillmair 1984; Cohen & Jones 1987; Le Bertre 1990; Le Bertre & Lequeux 1993). Although these absorptions could arise in the diffuse interstellar medium, likely much of it arises in the circumstellar environment. While not all such

[1] Space Science Division, NASA-Ames Research Center, Moffett Field, CA 94035-1000.
[2] Peyton Hall, Princeton University Observatory, Princeton, NJ 08544.

C-rich objects show strong DIBs in their spectra, this nevertheless implies that the carrier of these DIBs is carbonaceous in nature. Some of these objects are bright in the IR emission features at 3.3, 6.2, 7.7, and 11.3 μm attributed to polycyclic aromatic hydrocarbons (PAHs) and related aromatic materials. Recently, it was recognized that a few of the emission features in the visible spectrum of the Red Rectangle occur at wavelengths very close to those of some DIBs (Fossey 1990, 1991; Sarre 1991; Scarrott et al. 1992). This carbon-rich object is presumably a protoplanetary nebula in which the central star illuminates gas and dust ejected during the preceding asymptotic giant branch phase. These emission features have now also been detected in the spectrum of V 854 Cen, an R CrB star (Rao & Lambert 1993). R CrB stars are also C-rich and surrounded by recently ejected dust envelopes. While they are also noted for their H-deficiency, this particular R CrB star shows strong Balmer emission lines (Rao & Lambert 1993). Thus, again, these observations strongly imply a (hydro)carbon carrier for the DIBs.

Although the DIBs were discovered in the third decade of this century (Heger 1922) and their interstellar origin was recognized in the 1930s (Merrill 1934), the carrier (or carriers) of the DIBs is still unknown. Indeed, even the question of whether the carrier(s) are molecular or solid state in origin is still a matter of dispute. For example, from the study of the Taurus dark cloud complex, Snow & Seab (1991) argue for a molecular origin for the diffuse bands while Adamson, Whittet, & Duley (1991) find evidence for the formation of the DIBs in impurity centers in mantled grains. Recent observations and theory tend, however, to lean toward a molecular origin for the diffuse bands (Herbig 1993). To a large extent this is a problem inherent in structured electronic transitions which are very characteristic for specific species or materials. While this gives electronic transitions great identification powers a posteriori, in the absence of other knowledge, a priori an almost limitless number of specific species has to be investigated in the laboratory. Possible carriers have therefore almost exclusively been proposed based upon independent knowledge and/or guesswork of their importance in the interstellar medium. This includes unsaturated carbon chain molecules and PAH molecules which are thought to be present based upon millimeter and infrared observations, as well as C_{60} and other fullerenes because of their molecular elegance.

In this paper we reexamine the suggestion, made a decade ago, that ionized PAH molecules are the carriers of the DIBs (Allamandola, Tielens, & Barker 1985; van der Zwet & Allamandola 1985; Léger & d'Hendecourt 1985; Crawford, Tielens, & Allamandola 1985). This "comeback" has largely been motivated by the promising results recently obtained from preliminary laboratory studies of isolated, ionized, PAHs (Salama & Allamandola 1991a, b, 1992a, b) which permit a more in-depth assessment of the PAH-DIB proposal. The focus of the study is on two aspects of the PAH-DIB hypothesis. First, the conditions in the diffuse interstellar medium are expected to produce a mixture of neutral as well as positive and negative PAHs (Bakes & Tielens 1994). The relative proportions of each depend on the physical conditions (i.e., density, incident UV field) in the cloud(s) along the line of sight, as well as on the specific properties such as ionization potential and electron affinity of the particular PAHs under consideration. Second, associated with these different ionization states, any PAH can have three distinctly different spectroscopic identities. Taken together, these aspects can produce variations in the spectral behavior among different lines of sight which are similar to those observed for the DIBs.

We realize that positive identification requires extensive, appropriate, laboratory studies, and here too significant advances have recently been made (Salama & Allamandola 1991a, b, 1992a, b, 1993; Ehrenfreund et al. 1992a, b, 1995; Salama, Joblin & Allamandola 1994, 1995; Léger, d'Hendecourt, & Défourneau 1995). Our main goal here is to delineate the large number of PAH species and their ionization stages possible in the diffuse ISM. This will allow a more concerted laboratory attack on this problem. Moreover, even if PAHs were not the carrier, very similar considerations would apply to any other molecular carrier postulated for some of the DIBs and hence the formalism developed in this paper will be useful as well.

This paper is organized as follows. Section 2 describes the PAH charge distribution as a function of PAH size, structure, and ionization properties as well as interstellar environment. The UV and visible-to-near-infrared spectroscopic properties of PAHs are discussed in terms of PAH size, structure, and charge state (neutral, cationic, and anionic forms) in § 3. The salient features of PAH spectral properties are summarized in the Appendix. The constraints developed in these two sections are applied to the PAH/DIB hypothesis in § 4. Finally, the conclusions are summarized in § 5.

2. THE CHARGE DISTRIBUTION OF INTERSTELLAR PAHS

2.1. *Model*

The charge of interstellar PAHs reflects the balance between ionization by photons and by charge exchange on the one hand and collisional recombination with electrons and ions on the other hand (Draine & Sutin 1987; Bakes & Tielens 1994). Under the conditions reigning in the diffuse interstellar medium, charge exchange of C^+ and other ions with neutral PAHs is about two orders of magnitude less important than photoionization and we have, thus, neglected this process. The relative importance of the other processes under consideration is regulated by molecular properties of the species under consideration (i.e., ionization potential, electron affinity, ionization yield, and electron sticking coefficient) as well as the physical conditions in the interstellar medium (i.e., electron density and incident UV field). For small PAHs, the molecular properties are amenable to direct laboratory measurement and several species have been studied in detail in the laboratory (Leach 1987, 1989; Verstraete et al. 1990; Tobita et al. 1992; Abouelaziz et al. 1993). Experimental studies indicate that, for larger species, these properties can be reasonably well determined by extrapolation (see Burtscher 1992). For conditions typical of the diffuse interstellar medium, PAHs have several accessible charge states. For PAHs with less than 25 C atoms these are limited to neutral and plus or minus one electron. Larger species can progressively acquire more positive and negative charges (Bakes & Tielens 1994). In this section, we will calculate the charge distribution for several PAHs and small grains under various interstellar conditions.

Using the formalism of Bakes & Tielens (1994), we have solved the ionization balance for the charge distribution of several PAH molecules and small graphitic grains in the diffuse interstellar medium (ISM). For the smaller PAH molecules, we selected pyrene ($C_{16}H_{10}$), pentacene ($C_{22}H_{14}$), and coronene ($C_{24}H_{12}$). For the small graphitic grains, we considered a disk-shaped grain composed of $N_c = 100$ carbon atoms and a

TABLE 1

PHYSICAL PROPERTIES OF POLYCYCLIC AROMATIC HYDROCARBONS AND SMALL GRAPHITIC GRAINS.

Molecule	EA_1 (eV)	IP_1 (eV)	s_e ($Z = 0$)	J_{pe} ($Z = 0$)	J_{pe} ($Z = -1$)	J_e ($Z = 0$)	J_e ($Z = +1$)
Pyrene ($C_{16}H_{10}$)[a]	0.55	7.41	10^{-3}	3.95×10^{-9}	3.95×10^{-9}	5.30×10^{-12}	1.30×10^{-8}
Pentacene ($C_{22}H_{14}$)[a].....	1.10	6.74	1	5.36×10^{-9}	5.36×10^{-9}	6.76×10^{-9}	1.30×10^{-8}
Coronene ($C_{24}H_{12}$)[a]	0.64	7.36	10^{-3}	5.83×10^{-9}	5.83×10^{-9}	7.22×10^{-12}	1.30×10^{-8}
$N_C = 100$[b]	3.14	5.66	1	1.74×10^{-8}	4.26×10^{-8}	2.14×10^{-8}	4.42×10^{-7}
$N_C = 1000$[b]	3.84	4.96	1	2.15×10^{-7}	2.73×10^{-7}	3.74×10^{-8}	6.37×10^{-7}

NOTE.—Table lists the PAH, its first electron affinity (EA_1), first ionization potential (IP_1) and the electron sticking coefficient (s_e) in the first four columns. The last four columns list the photoelectric ejection rate (J_{pe}) for neutral and negatively charged PAHs and the PAH-electron recombination rate (J_e) for neutral and positively charged PAHs. The rates are calculated under conditions typical for the diffuse ISM, such that $n_e = 7.5 \times 10^{-3}$ cm^{-3}, $T = 100$ K, and $G_o = 1$.

[a] EA_1 and IP_1 data are from Leach 1987; J_e ($Z = +1$) are calculated using the electron recombination rate measured by Abouelaziz et al. 1993.

[b] EA_1 and IP_1 data are from Bakes & Tielens 1994; J_e ($Z = +1$) are calculated using the theoretical data from Draine & Sutin 1987.

spherical grain of $N_c = 1000$. The physical properties of these species are summarized in Table 1 whereas some representative PAH structures are shown in Figure 1. The measured ionization cross section per C atom is very similar for pyrene and coronene (Verstraete et al. 1990). We have scaled the ionization cross section of pentacene and the small graphitic grains according to their number of C atoms. For the PAH molecules, we have used experimentally measured electron affinities and ionization potentials (Leach 1987, 1989; Tobita et al. 1992). The ionization potentials for the grains were calculated using electrostatics, adopting a work function for bulk graphite of 4.4 eV (Smith 1961; Gallegos 1968). This approach yields good agreement with experimental ionization potentials of PAH molecules, small graphite grains, as well as bulk graphite (Smith 1961; Bakes & Tielens 1994). The electron sticking coefficient for neutral PAHs is a strong function of their electron affinity. Both coronene and pyrene have small electron affinities ($\approx$0.6 eV) and hence low sticking coefficients ($S[e] \approx 10^{-3}$; Allamandola, Tielens, & Barker 1989). Pentacene, on the other hand, was selected because of its higher electron affinity (1.1 eV) and its resulting high electron sticking coefficient ($S[e] = 1$). The grains will have electron sticking coefficients of unity as well.

For our standard model of the physical conditions in the diffuse ISM, we adopted a gas temperature, $T_g = 100$ K; hydrogen nucleus density, $n_H = 25$ cm^{-3}; electron fraction of 3×10^{-4} (i.e., electron density, n_e, of 7.5×10^{-3}); and the average interstellar FUV radiation field, $G_o = 1$, corresponding to 1.6×10^{-3} ergs cm^{-2} s^{-1} (10^8 photons cm^{-2}; Habing 1968). The hydrogen nucleus density and the FUV absorption cross section were varied in order to ascertain the effects on the grain charge. The results are described below.

2.2. *Results*

Figure 2 and 3 show the calculated charge distributions as a function of the hydrogen density. Some insight can be gained by considering a species with two charge states, 0 and +1, which is quite appropriate for small compact PAHs such as

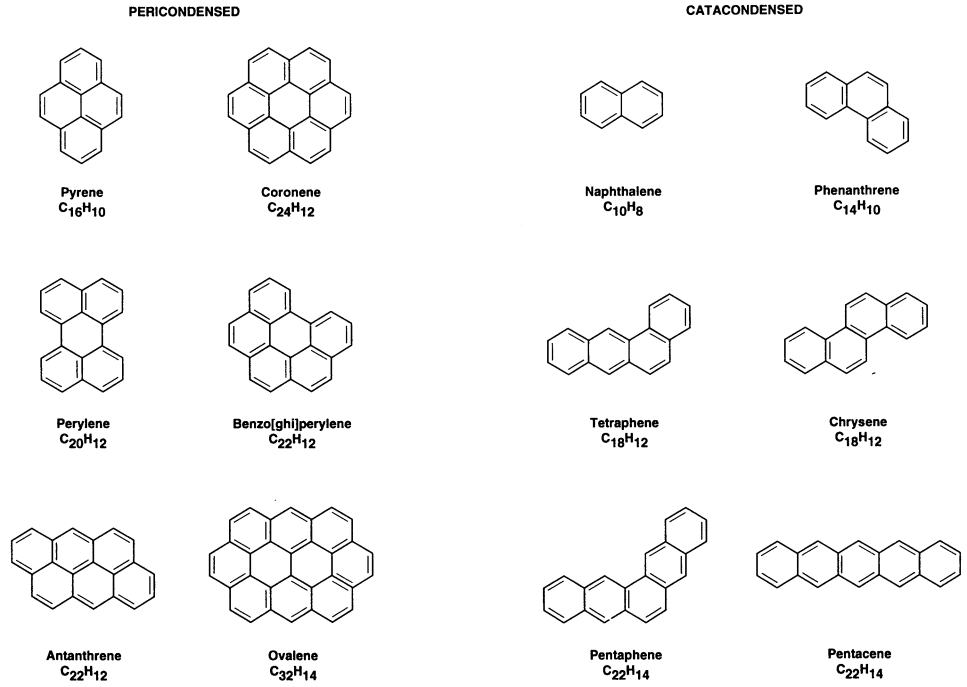

FIG. 1.—Structures of some representative pericondensed and catacondensed polycyclic aromatic hydrocarbons (PAHs). Hydrogen atoms, located on the periphery, are not represented.

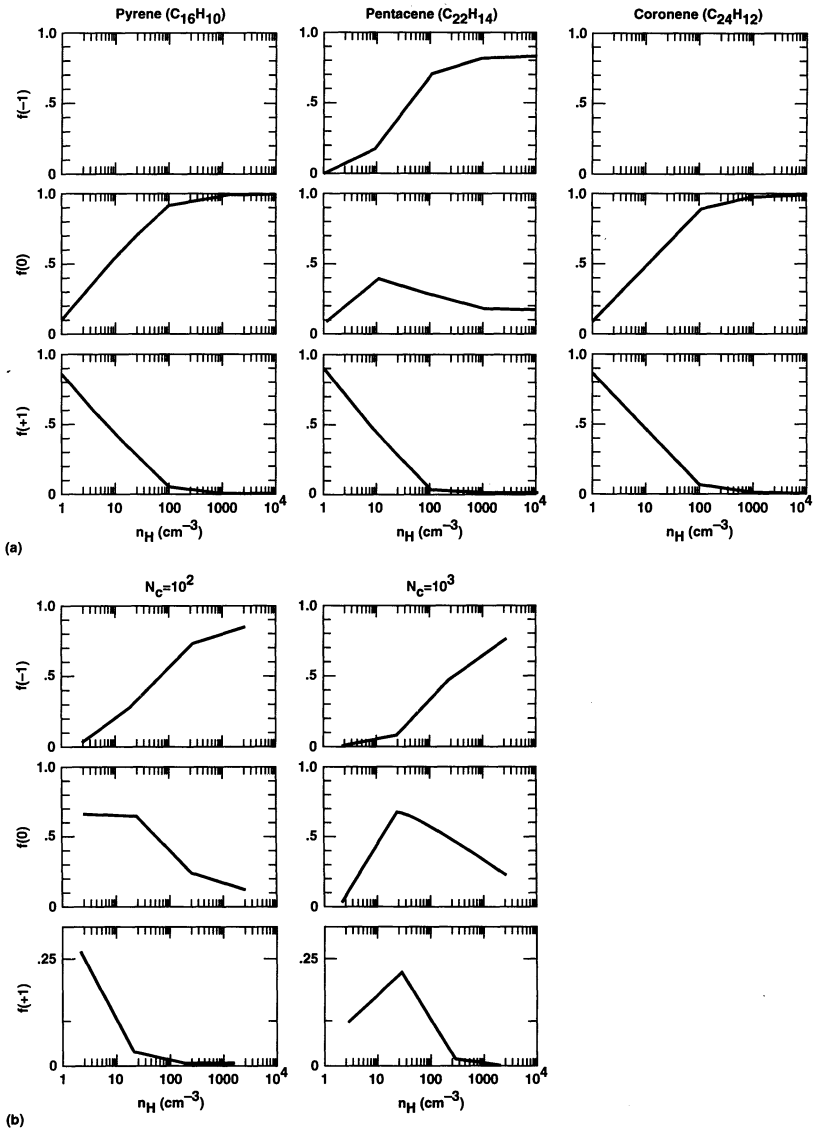

FIG. 2.—Charge distribution of some PAHs (pyrene, pentacene, and coronene) and small grains ($N_C = 10^2$; $N_C = 10^3$) as a function of the hydrogen density (n_H). Physical conditions: $T_{gas} = 10^2$ K and $G_o = 1$. PAH cation electron recombination rates (J_e [$Z = +1$]) are calculated using the experimental dissociative recombination rate of $C_6H_6^+$ (10^{-6} cm^3 s^{-1}) taken from Abouelaziz et al. (1993).

coronene and pyrene. Then, the neutral fraction, $f(0)$, is given by (Bakes & Tielens 1994)

$$f(0) = (1 + J_{pe}/J_e)^{-1}$$
$$= [1 + (6.6 \times 10^{-7})(N_c\, G_o\, T^{1/2})/n_e]^{-1}\,, \quad (1)$$

where J_{pe} is the neutral photoelectric ionization rate ($\approx 2 \times 10^{-10}\, N_c\, G_o$ s^{-1}) and J_e the electron recombination rate ($1 \times 10^{-6}(300/T)^{1/2} n_e$ s^{-1}). This relation shows that the neutral fraction increases as the electron density increases or the UV field intensity decreases. Also, when the size (i.e., the number of carbon atoms) increases, the UV absorption cross section increases and the neutral fraction decreases. Note that we have modified here the relation given by Bakes & Tielens (1994) to replace the electron recombination rate theoretically calculated for small grains (Draine & Sutin 1987) by a more realistic value derived from the experimental dissociative recombination rate of $C_6H_6^+$ measured at 300 K with an uncertainty of 30% (Abouelaziz et al. 1993). The charge state of small PAHs being sensitive to the values adopted for the recombination coefficient, the experimental recombination rates lead to the prediction of a higher fraction of positive PAH ions compared to the case where the theoretical rate is used. Thus, in the case of pyrene and coronene, the fraction of positive ions, $f(+1)$, is calculated to be on the order of 2% when using the theoretical electron recombination rate (Draine & Sutin 1987) while it increases up to 30%–35% (Fig. 2) and 60%–70% (Fig. 3) when using the laboratory measured electron recombination rates of $C_6H_6^+$ (1×10^{-6} cm^3 s^{-1}) and $C_{10}H_8^+$ (3×10^{-7} cm^3 s^{-1}), respectively (Abouelaziz et al. 1993). *In all cases, however, the distribution of small compact PAHs is found to be limited to only two charge states* (*neutrals* [0] *and cations* [+1]).

Because the electron sticking efficiency of neutral coronene and pyrene is so low, the fractional abundance of these PAH anions is always very small if not negligible. Hence, their

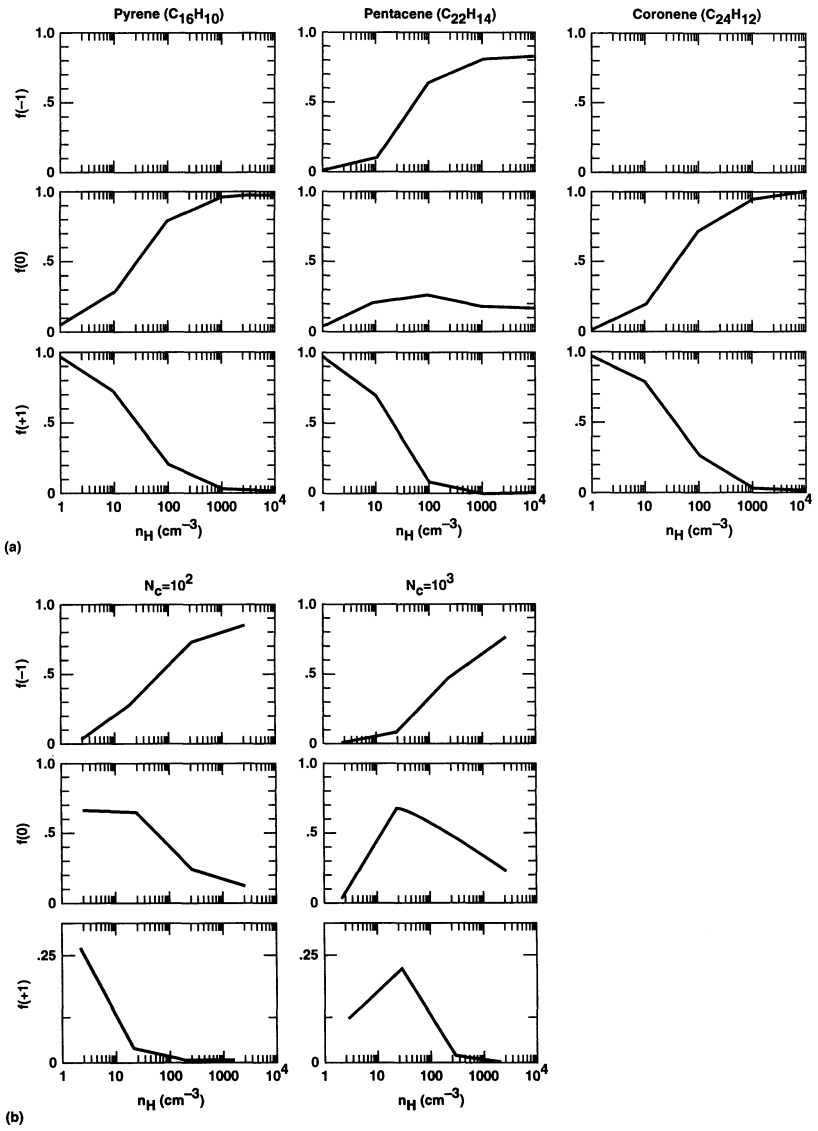

FIG. 3.—Charge distribution of some PAHs (pyrene, pentacene, and coronene) and small grains ($N_C = 10^2$; $N_C = 10^3$) as a function of the hydrogen density (n_H). Physical conditions: $T_{gas} = 10^2$ K and $G_o = 1$. PAH cation electron recombination rates (J_e [$Z = +1$]) are calculated using the experimental dissociative recombination rate of $C_{10}H_8^+$ (3×10^{-7} cm^3 s^{-1}) taken from Abouelaziz et al. (1993).

charge distribution is well described by equation (1). In contrast, for pentacene and larger species, three or more charge states are accessible and anions dominate at high electron densities. However, except for large species at high densities, the charge distribution is dominated by only two charge states at any one time albeit that the actual charge states involved will vary with the physical conditions. As a result, the charge distribution can still be described by relations analogous to equation (1), despite the fact that the actual charge states involved can vary from species to species and with the physical conditions in the region. Thus, in general, any species becomes less positively charged with increasing electron density (Figs. 2 and 3). Similarly, decreasing the incident UV field or increasing the UV optical depth (i.e., depth in the cloud) will lead to higher neutral and/or anion abundances.

The effect of increasing grain size is best studied by comparing the results for $N_C = 10^2$ with those for $N_C = 10^3$ (Figs. 2 and 3). The ionization rate increases with the volume of the species, while the recombination rate increases only linearly with grain size due to Coulomb focusing. As a result, under the same physical conditions, larger species are more positively charged than smaller species, a trend which is readily apparent in Figures 2 and 3. While these calculations have concentrated on the electron density as the physical variable, similar results are obtained for varying FUV intensity and gas temperature (see eq. [1]). Finally, measured UV absorption cross sections per C atom of individual PAH species vary by about a factor of 2 from one species to another. Essentially, this will shift the curves in Figures 2 and 3 to lower or higher density without changing their shape (see eq. [1]).

2.3. *Cloud Model*

To illustrate the variation expected within a single cloud, we have calculated the charge distribution as a function of depth for the well-studied cloud along the line of sight toward ζ per. We have adopted model F from van Dishoeck & Black (1986) for the density, electron fraction, temperature, and UV extinction as a function of depth. This model fits the various atomic

and molecular line observations toward this source well. The results for pentacene, pyrene, coronene, and $N_C = 100$ are shown in Figures 4 and 5. In line with the results described above, for the conditions in this cloud, pentacene molecules which are distributed among three charge states $(-1, 0, +1)$ at the surface of the cloud become approximately half neutral and half negatively charged with increasing depth in the cloud. A similar effect is observed for $N_C = 100$ species which are predominantly neutral at the surface of the cloud. In contrast, coronene and pyrene which are predominantly positively charged at the surface of the cloud become predominantly neutral with increasing depth in the cloud. As expected, the charge distribution shifts toward less positively charged species with increasing depth into the cloud as a result of the increased density (i.e., recombination rate) and the decreased UV field (ionization rate).

2.4. *Conclusions*

In summary, for typical conditions in diffuse interstellar clouds:

1. For small, compact PAHs having electron affinities less than about 0.6 eV (i.e., small electron sticking coefficients), cations will always contribute significantly to the total distribution ($\frac{1}{3}$ to $\frac{2}{3}$ depending on the electron recombination rate involved). The rest of the distribution will consist of neutrals since the fraction of anions is always negligible.

2. Small, non-compact PAHs like pentacene with high electron affinities will be roughly equally distributed between neutral species, negative and positive ions (up to 30%–50% of cations depending on the electron recombination rate involved).

These findings contrast with the conclusions of a previous study (Bakes & Tielens 1994) which used a theoretical electron-PAH cation recombination rate which was too high.

3. Larger, planar PAHs will be predominantly neutral ($\frac{2}{3}$) with a substantial fraction of anions ($\frac{1}{3}$). The contribution of cations to the distribution will be negligible.

4. Species much larger than 100 C atoms will again have a considerable fraction in the positively charged state (about $\frac{1}{3}$) and the rest in the neutral form.

We note therefore that, if, as argued in § 3, *small compact PAH ions are the carriers of (some of) the DIBs, their visual absorption is possibly due to their cationic state, not their anionic state* as illustrated by recent experimental findings (Salama & Allamandola 1992a, b; Salama et al. 1995).

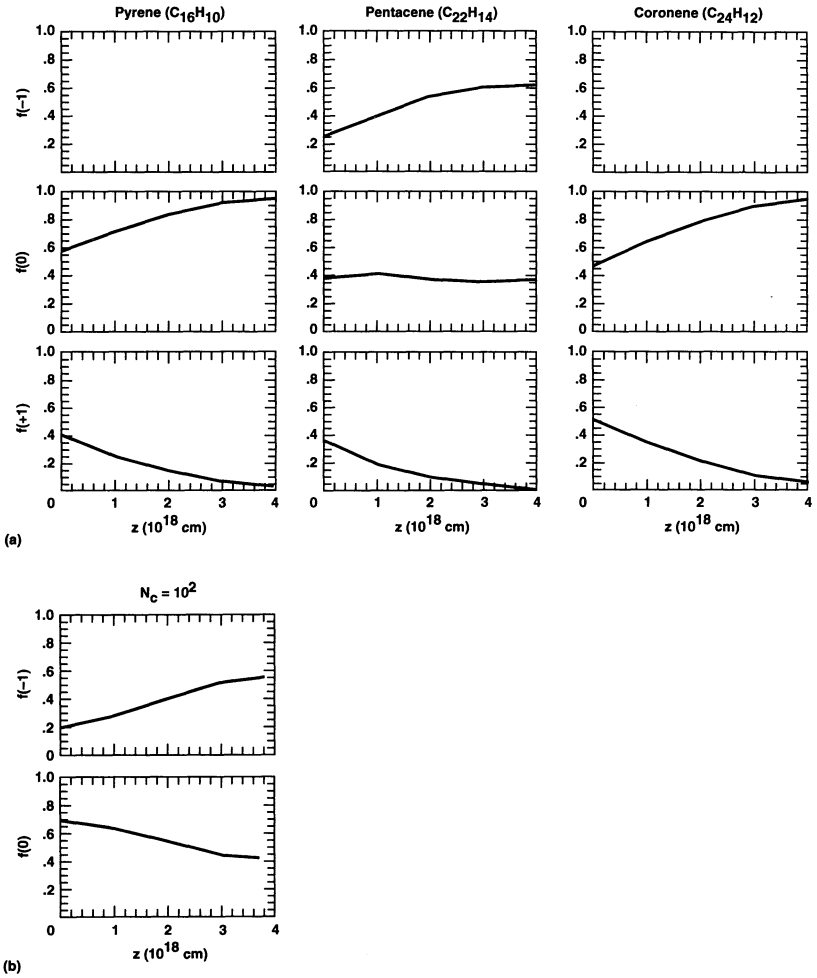

FIG. 4.—Variation of PAHs (pentacene, pyrene, and coronene) and small grains ($N_C = 10^2$) charge density as a function of depth inside the molecular cloud ζ per. Physical conditions: $T_{gas} = 10^2$ K, $n_H = 25$ cm^{-3}, and $G_o = 6$ at the surface. PAH cation electron recombination rates (J_e [$Z = +1$]) are calculated using the experimental dissociative recombination rate of $C_6H_6^+$ (10^{-6} cm^3 s^{-1}) taken from Abouelaziz et al. (1993).

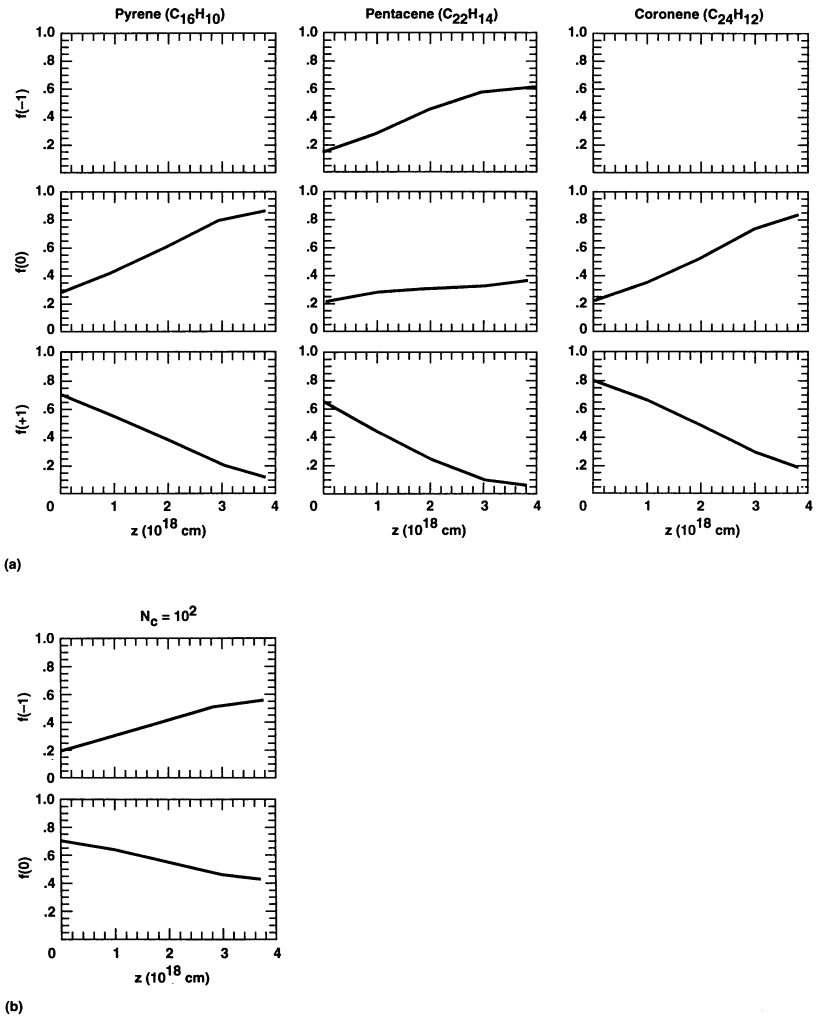

FIG. 5.—Variation of PAHs (pentacene, pyrene, and coronene) and small grains ($N_C = 10^2$) charge density as a function of depth inside the molecular cloud ζ per. Physical conditions: $T_{gas} = 10^2$ K, $n_H = 25$ cm^{-3}, and $G_o = 6$ at the surface. PAH cation electron recombination rates (J_e [$Z = +1$]) are calculated using the experimental dissociative recombination rate of $C_{10}H_8^+$ (3×10^{-7} cm^3 s^{-1}) taken from Abouelaziz et al. (1993).

3. SPECTROSCOPIC PROPERTIES OF PAHS

Quantum chemical considerations are used here to examine the general spectroscopic properties of PAHs in their neutral and ionized forms (see Appendix for a detailed discussion of the spectroscopy and photophysics of neutral and mono-ionized PAHs. A discussion of the physical and chemical properties of PAHs can be found in Leach 1987, 1989). Of particular importance is the systematic classification of these properties as a function of the structure of the molecules (size and/or shape) and, hence, to derive some general criteria for the selection of relevant candidates for the DIBs. The principal questions can be phrased as follows.

1. How does the absorption wavelength shift with the size and/or the symmetry of the molecule?
2. How does the absorption spectrum change with charge state?
3. Which transitions are strong (optically allowed) and which are weak (optically forbidden)?
4. Can one associate the finite wavelength domain where most of the DIBs are observed (4000–9000 Å range) to a specific size and/or structure range of PAHs?

3.1. *Neutral PAHs*

Neutral PAHs have three (sometimes four) well-defined absorption band systems (α, p, β, and β'; Clar 1964) in the near-ultraviolet (NUV) and visible spectral regions (Fig. 6). The absorption band systems are associated with transitions in the π electron system of the molecule (Fig. 7*a*; see Appendix).

Here, we will use a general formula which is applicable to *all* classes of PAHs to estimate the absorption edge of any PAH, independent of its structure. In this formula, empirically derived from a large set of experimental data (Streitwieser 1961), the energy of the first allowed electronic transition (i.e., the "p" band in Clar's terminology) is linearly related to the energy of the highest occupied molecular orbital (HOMO) through the relation:

$$\nu_p(\mathrm{cm}^{-1}) = (38040 \pm 660) m_{\mathrm{HOMO}} + (10520 \pm 340)\,, \quad (2)$$

where ν_p is the wavenumber of the "p" band, and m_{HOMO} is the energy of the HOMO given in units of β ($\beta = -2.9$ eV is the resonance integral which expresses the interaction between the π orbitals of neighboring carbon atoms). This relation has been verified for alternant hydrocarbons such as PAHs for which

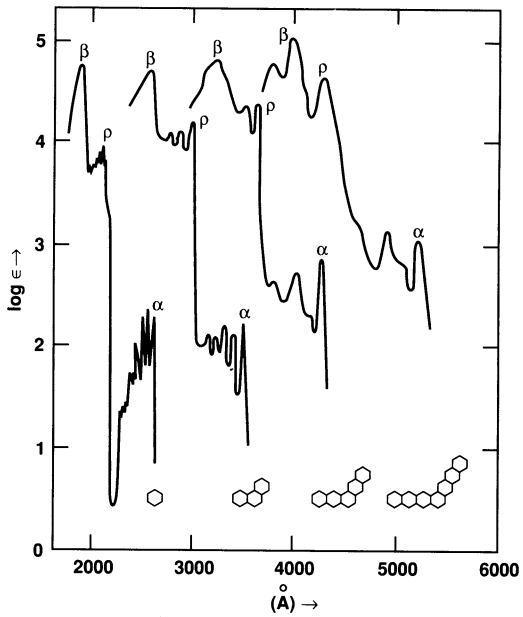

FIG. 6.—Absorption spectra of some representative small catacondensed neutral PAHs. Band notations refer to Clar's classification. Taken from Birks (1970).

m_{LUMO}[3] is the negative of m_{HOMO} (see Fig. 7). Note, however, that the "p" band is sometimes preceded by the very weak electronic transition α which may shift the absorption edge to a slightly lower energy. Combining, now, equation (2) with the calculated density of states of π-bonded clusters (Robertson 1986) and taking into account the simple relation between the band gap energy (E_g) of a cluster of fused benzenoid rings and its HOMO energy ($m_{HOMO} = E_g/2\beta$), one can derive the absorption edge of any PAH comprised of fused benzenoid rings (Fig. 8). For example, a hypothetical compact cluster ($E_g = 2|\beta|M^{-0.5}$, where M is the number of fused benzenoid rings) comprised of 100 benzenoid rings (about 250–300 C atoms) will exhibit its first allowed transition near 7000 Å while the same transition would occur around 9200 Å for a 10^4 benzenoid ring cluster (i.e., at the graphite limit, about 3×10^4 C atoms). In this latter case, however, the energy level separation within the π system (≈ 6 eV/N_C where N_C is the number of carbon atoms in the molecule) is less than the thermal energy at 10 K and the absorption will resemble a continuum.[4] In contrast, a compact PAH comprised of eight rings (20–30 carbon atoms) or less will absorb only at wavelengths shorter than 4000 Å. In the case of linear PAH molecules, where the energy gap decreases more rapidly with the molecular size (E_g is now proportional to M^{-2} instead of $M^{-0.5}$), a row of only 30 fused benzenoid rings will begin to absorb near 9200 Å.

Hence, for the purpose of this study, we can conclude that *small neutral PAHs (i.e., containing less than 20–30 carbon atoms) absorb only in the UV ($\lambda < 4400$ Å) and cannot contribute to the known DIBs.* Larger compact PAHs ($30 \leq N_C \leq 10^4$) will absorb in the visible and NIR regions and could contribute to the DIBs. For example, if the well-known 4430, 5780, and 6284 Å DIBs were due to neutral compact PAHs, the implied size of these PAHs would be of the order of 10, 40, and 60 fused benzenoid rings, respectively (see Fig. 8). In the case of very large PAHs (i.e., macromolecules or "graphitic" plates containing more than 10^4 carbon atoms), the transitions will merge into a continuum extending throughout the visible and infrared and, thus, are not related to the discrete diffuse bands. The corresponding upper limit constraint for rows of linear PAHs (less relevant for astrophysical applications because of their lower stability) is 25 to 30 ring molecules.[5]

3.2. *PAH Ions*

In the case of ionized PAHs, the situation is more complicated than for the neutrals due to the new electronic transitions which are induced in the π system by the removal (cations) or addition (anions) of an electron (see Appendix). A schematic representation of the molecular levels, together with the corresponding classification of the monoelectronic transitions (types I, A, and B), are shown in Figures 7*b* and 7*c*.

Few experimental data are available on the spectroscopy of charged PAHs making it difficult to derive general conclusions. The general conclusions one can draw, however, from the survey of the available literature on the spectroscopy of PAH ions (cf. Appendix) are as follows.

1. Monocations and monoanions absorb in the visible and NIR regions as well as in the UV *and thus could contribute to the DIBs.*
2. Monocation and monoanion absorption spectra resemble each other with the cation transitions generally blueshifted with respect to those of the anion.
3. Monocation and monoanion absorption onset (type I transitions) shift to longer wavelengths as the number of benzenoid rings increases (i.e., the size increases).
4. In the case of small PAHs, type I transitions are responsible for most (if not all in some cases) of the visible bands of the ions.
5. The lowest energy transition (generally of type I) is optically forbidden in the case of highly symmetric molecular ions (anions and cations beonging to point-group symmetry (D_{2h}, C_{2h}...).
6. In the case of large PAHs (molecules containing more than 300 carbon atoms), transitions of the ion merge into a continuum.[6]

More specific conclusions can be drawn, however, in the case of the more stable compact PAHs. From a survey of the electronic spectra of pericondensed PAH cations, Khan (1991) noted that the A bands are the most intense in the lower energy region of the spectrum (i.e., visible–NIR range). The same phenomenon is observed for pericondensed PAH anions (Shida &

[3] LUMO stands here for the lowest unoccupied molecular orbital.

[4] Note that the strength of the Hückel molecular orbital (HMO) theory implicitly used here is that it is the *only* molecular orbital theory to converge to the correct graphite limit, i.e., it is equally applicable to small PAH molecules as well as the larger PAH molecules that make up graphitic substances (Stein & Brown 1991).

[5] Almost no information is available—whether from experimental and/or theoretical studies—for neutral PAH derivatives resulting from H atom abstraction or addition. These neutral radicals are also of astrophysical interest. Recently, however, theoretical calculations of the electronic spectra of naphthalene ($C_{10}H_8$) and its derivatives ($C_{10}H_7$ and $C_{10}H_9$) have been performed (Du, Salama, & Loew 1993). These semiempirical calculations indicate that, like their parent molecule, the dehydrogenated derivatives do not absorb in the visible and, hence, cannot contribute to the DIBs. However, the hydrogen *addition* derivatives do show electronic absorption in the visible and could, if present, contribute to the DIBs.

[6] Semiempirical calculations of the electronic spectra of the monoanions of naphthalene ($C_{10}H_8$) and its derivatives resulting from H atom abstraction or addition ($C_{10}H_7$ and $C_{10}H_9$) indicate that these derivatives also exhibit electronic absorption in the visible–NIR range and could, if present, contribute to the DIBs (Du, et al. 1993).

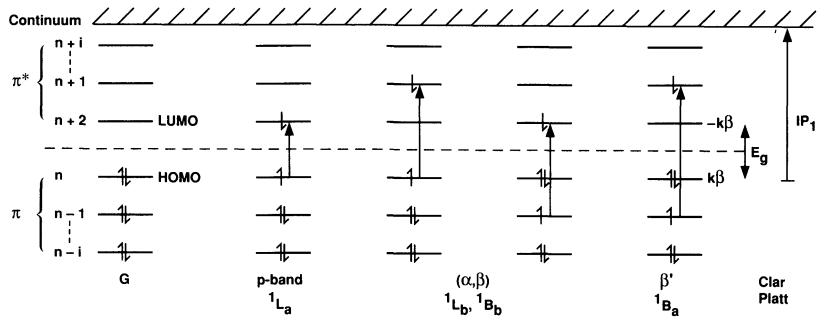

FIG. 7*a*

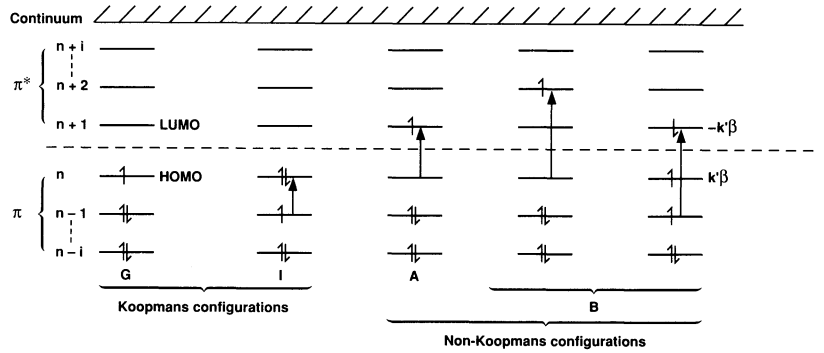

FIG. 7*b*

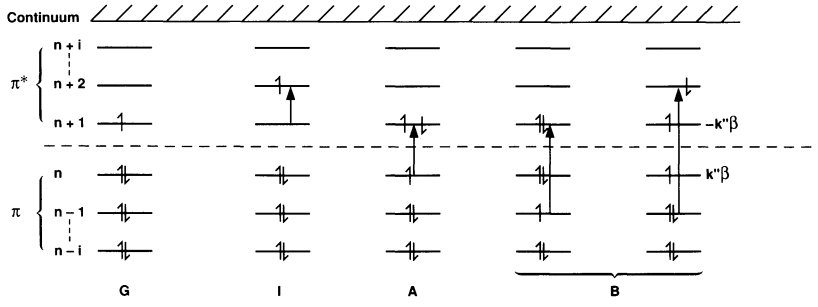

FIG. 7*c*

FIG. 7.—Hückel π molecular orbital energy level diagrams for (*a*) neutral, (*b*) monocation, and (*c*) monoanion PAHs. Only one-electron excitations, represented by the filled arrows, are represented. G corresponds to the ground electronic state configuration. E_g is the gap energy, IP_1 the first ionization potential, k, k', and k'' are constants, and β the resonance integral (see text). Open arrows picture electrons.

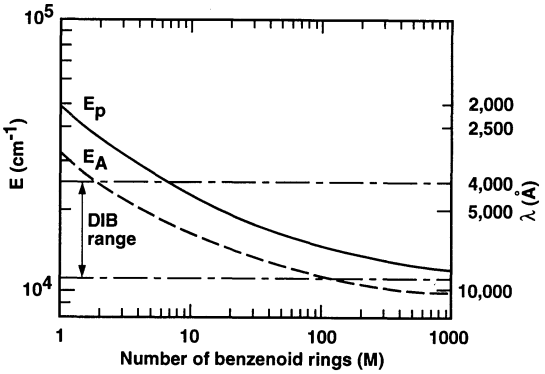

FIG. 8.—Neutral (E_p; *solid line*) and ionized (E_A; *dashed line*) compact PAH band energy as a function of the number of benzenoid rings (M) in the molecular structure. Note the E_p corresponds to the absorption edge of the neutral molecule while E_A represents the strongest absorption of the ion. The region between the two dash-dot lines encompasses the energy region where most of the known DIBs fall (i.e., 4000–9000 Å [11,000–25,000 cm^{-1}]).

Iwata 1973). Although the ion A bands bear in common with the neutral *p* bands the fact that they both involve transitions between the HOMO and LUMO orbitals, their energy is shifted due to a variation in the π-electron interaction term between the neutral and the monoion (see Appendix and Fig. 7).[7] A survey of experimental data (Khan & Schmidt 1985; Khan, Husain, & Haselbach 1993) shows, moreover, that the empirical relation

$$E_A(\mathrm{cm}^{-1}) = (2580 \pm 1613) + 0.60E_p \qquad (3)$$

where E_A and E_p are the energies, in cm^{-1}, of the cation A bands and neutral p bands, respectively, holds for catacondensed *and* pericondensed PAHs. We have shown, above, that E_p can be estimated for any given size neutral PAH through its calculated band gap energy, E_g (eq. [2]). Combining equations

[7] In a first approximation (i.e., neglecting the configuration interaction), the relation between the cation A band and the neutral *p* band energies can be expressed as $E_A = E_p - K_{mn}$, where K_{mn} represents the exchange term.

(2) and (3), and assuming that the energy difference between the cation and anion spectral A bands is small, we can now derive the size range of compact PAH ions which may contribute significantly to the DIBs (i.e., possess an A band in the range 4000–9000 Å). It is found that *only compact PAH ions of less than 100 fused benzenoid rings (250 carbon atom molecules) could contribute to the DIBs* (see Fig. 8). For example, in this hypothesis, the well-known 4430, 5780, and 6284 Å DIBs would be associated with PAH ions of 4, 7, and 10 fused benzenoid rings, respectively. Large compact PAH ions containing more than 100 rings may have absorption bands in the DIB range but these bands (types I and B) are weak compared to the A band and can be neglected in a first approximation to derive molecular size constraints. (Note that this approximation holds for compact PAH ions only because their NUV-NIR spectrum is clearly dominated by the A band. This is not true for noncompact PAH ions).

3.3. *Conclusions*

In conclusion, surveying the ultraviolet, visible, and near-infrared spectroscopic characteristics of compact PAHs (considered as the most probable PAH species to survive in the diffuse ISM environment due to their higher stability) it is found that:

1. For neutral PAHs, molecules containing from 30 carbon atoms up to graphitic-type benzenoid ring clusters (containing about 1.0×10^4–3.0×10^4 C atoms) could, if present, contribute to the DIBs.
2. For singly ionized PAHS (cations and anions), the situation is drastically different since *only* molecular ions with less than about 250 carbon atoms could, if present, significantly contribute to the DIBs.

4. POLYCYCLIC AROMATIC HYDROCARBONS AND THE DIFFUSE INTERSTELLAR BANDS

In the following, the general PAH properties described in §§ 2 (charge state) and 3 (photophysics) are used to derive further insights into the conditions which must be met if PAHs are to account for some of the DIBs. This general approach is adopted since it will be some time before an adequate spectral database of isolated PAHs in their neutral, cationic, and anionic forms exists in order to fully assess the merits of the PAH/DIB hypothesis.

4.1. *Abundance Constraints*

In this section an estimate is made of the column densities of carriers required to provide the total equivalent width of the diffuse interstellar bands. First the equivalent widths (W_λ) of the DIBs are considered. These are then evaluated in terms of PAH number densities required and percent of cosmic carbon consumed, and this is compared to PAH abundances derived from IR observations.

There are some 50 strong and moderately strong DIBs tabulated in Herbig (1975) toward the star HD 183143. These bands, listed in Table 2, form the basis of our analysis. Although many new bands have been added to the list of known DIBs (Herbig 1988; Herbig & Leka 1991; Sanner, Snell, & Vanden Bout 1978; Jenniskens & Désert 1994), those in Table 2 include the strongest, and would dominate the total equivalent width (the bands listed in Table 2 represent a total equivalent width [W_λ] of 20.9 Å to compare to the 26.3 Å equivalent width associated with *all known* DIBs in the 4000–9000 Å range). For the following analysis, the band equivalent widths are characterized as strong ($W_\lambda \geq 1$ Å), moderate (1 Å $> W_\lambda \geq 0.1$ Å), or weak ($W_\lambda < 0.1$ Å). This analysis assumes that each DIB is produced by *one* PAH.

TABLE 2

DIFFUSE INTERSTELLAR BAND WAVELENGTHS (λ) EQUIVALENT WIDTHS (W_λ) AND ABUNDANCE[a]

λ (Å)	W_λ (Å)	N_{PAH}/N_H	λ (Å)	W_λ (Å)	N_{PAH}/N_H
4176.....	0.42	2.8302e-09	6204.....	0.22	6.7385e-10
4430.....	2.49	1.4825e-08	6207.....	0.15	4.5822e-10
4502.....	0.25	1.4825e-09	6270.....	0.12	4.0431e-10
4727.....	0.11	5.7951e-10	6281.....	1.44	4.3127e-09
4762.....	0.87	4.4474e-09	6284.....	0.71	2.6954e-09
4824.....	0.59	2.9650e-09	6315.....	0.39	1.1321e-09
4882.....	0.81	4.0431e-09	6359.....	0.76	2.6954e-09
4970.....	0.45	2.6954e-09	6379.....	0.12	4.0431e-10
5039.....	0.38	1.7520e-09	6413.....	0.10	2.8302e-10
5109.....	0.28	1.2534e-09	6451.....	0.48	1.3477e-09
5449.....	0.29	1.2129e-09	6494.....	0.19	5.3908e-10
5456.....	0.11	4.3127e-10	6532.....	0.62	1.7520e-09
5487.....	0.12	5.3908e-10	6614.....	0.33	8.8949e-10
5508.....	0.14	5.3908e-10	6939.....	0.35	8.4906e-10
5536.....	0.11	4.1779e-10	6993.....	0.17	4.0431e-10
5537.....	0.29	1.1051e-09	7224.....	0.33	8.0863e-10
5705.....	0.11	4.0431e-10	7357.....	0.22	5.3908e-10
5779.....	0.75	2.6954e-09	7432.....	0.65	1.3477e-09
5780.....	0.72	2.6954e-09	7569.....	0.27	5.5256e-10
5795.....	0.16	5.5256e-10	7651.....	0.11	2.6954e-10
5797.....	0.18	6.7385e-10	7709.....	0.54	1.0782e-09
5844.....	0.11	4.0431e-10	7928.....	0.50	9.4340e-10
6010.....	0.16	5.3908e-10	8038.....	0.11	2.6954e-10
6045.....	0.18	5.6604e-10	8621.1.....	0.13	2.6954e-10
6177.....	1.16	3.5040e-09	8621.2.....	0.31	5.3908e-10
6203.....	0.13	4.0431e-10	8648.....	0.23	4.0431e-10

NOTE.—This analysis is based on the strengths of the bands toward HD 183143, Herbig's standard DIB star with $E(B-V) = 1.26$ (Herbig 1975; Jenniskens & Désert 1994).

[a] Relative to cosmic hydrogen (N_{PAH}/N_H) abundance implied if PAHs are responsible for each DIB.

The column density (N) of material required to produce a DIB is given by the well-known relation (Spitzer 1978)

$$N = \frac{W_\lambda mc^2}{\lambda_0^2 f \pi e^2}, \quad (4)$$

where λ_0 is the wavelength, f the oscillator strength, and e^2/mc^2 the classical electron radius. An oscillator strength associated with the transition responsible for a given DIB must be assumed to evaluate N. For the strong and moderate interstellar DIBs we will use a value of $f = 0.13$, the value experimentally determined for the strongest transition (A band) of the pyrene cation, a good candidate for the 4430 Å DIB (Salama & Allamandola 1992b). For ions in general, the experimental results of Shida (1988) show that the peak molar extinction coefficients for the visible and near-infrared transitions of several specific PAH cations and anions fall within a factor of 2–3 of each other. However, the oscillator strengths of the strongest visible bands (Type I) of the naphthalene and phenanthrene cations isolated in neon are much smaller, approximately 500 times less than that for pyrene (Salama & Allamandola 1991a; Salama et al. 1994). In contrast, the oscillator strengths of the strongest visible transitions in neutral PAHs are close to 1, 10 times larger than the value adopted here.

There are only three strong DIBs toward HD 183143: the 4430, 6177, and 6281 Å bands. The total equivalent width

associated with these three bands is 5.09 Å. Using $f = 0.13$, the total abundance of the three different PAHs carrying these DIBs toward HD 183143 is 0.2×10^{-7} corresponding to a column density $N = 1.7 \times 10^{14}$ PAH$^+$ cm^{-2} (Table 2). Adopting a typical number of carbon atoms per PAH of 25–50, this corresponds to 0.3%–0.7% of the elemental carbon locked up in these three PAH ions. The equivalent widths of the moderately strong DIBs toward HD 183143 are also listed in Table 2. The total equivalent width of these bands is 15.83 Å. Again adopting an oscillator strength of 0.13, the inferred PAH abundance required to produce the total equivalent width of the moderate features is 0.6×10^{-7} (column density $N = 4.1 \times 10^{14}$ cm^{-2}), or about 1%–2% of the elemental carbon for 25–50 C atom PAHs.

These derived abundances are very sensitive to the adopted f-values. If we assume that the DIBs are carried by large (~ 50 carbon atoms), neutral PAHs ($f \sim 1$), only a few tenths of a percent of the elemental carbon is required. Approaching the problem of the strong ($W_\lambda \geq 1$ Å) and moderately strong (1 Å $> W_\lambda \geq 0.1$ Å) DIBs from the PAH point of view, the interstellar PAH abundance of 1% of the elemental C derived from the IR emission features (Allamandola et al. 1989) would correspond to an f-value of the order of 0.1. *This would tend to favor ions over neutrals since 0.1 is a typical f-value for the strongest (type A) transition of compact PAH ions.* As emphasized throughout, the strength of the DIBs is affected both by the oscillator strength and the abundance of the carrier. As an example, consider the strong 4430 Å DIB ($W/E[B-V] = 2.23$ Å) which has been attributed to a pyrene-like cation (Salama & Allamandola 1992b; Léger, d'Hendecourt, & Défourneau 1995). With a measured f-value of 0.13, the fraction of elemental C locked up in this carrier would be 0.2%. Likewise, if the weak 6742 Å DIB ($W/E[B-V] = 0.01$ Å) is due to $C_{10}H_8^+$, a noncompact PAH which has a measured f-value of only 4.0×10^{-4} for its strongest (type I) visible transition, 0.3% of the elemental C is consumed (Salama & Allamandola 1992a). Similarly, using the measured upper limits (50–100 mÅ/$E[B-V]$) for the bands at 4592 and 9466 Å for the coronene cation and 9783 Å for the ovalene cation and adopting f-values of 10^{-2} and 10^{-3} for the A and I transitions, respectively, upper limits of the order of 0.05% of the elemental carbon are derived for these PAH cations (Ehrenfreund et al. 1995). Interestingly, the upper limits in the abundance of these compact PAHs are smaller than those derived for the smaller PAHs, naphthalene and pyrene. This may relate to their relative stability under interstellar conditions (Ehrenfreund et al. 1995).

The possible distribution of strong and weak DIBs between compact and noncompact PAH ions, respectively, seems to be supported by recent experimental data (Salama et al. 1995). A survey of the experimental data suitable for comparison with astronomical data (i.e., spectra measured in neon matrices; see Appendix) shows that pericondensed PAH cations (such as pyrene, benzo[ghi]perylene, and coronene) with a strong type-A transition (oscillator strength, f, on the order of 0.1) which dominates the entire spectrum in the NUV to NIR range tend to correlate with strong, broad DIBs (normalized equivalent widths, $W/E[B-V]$, ranging from 0.3 to 2.0). On the other hand, catacondensed PAHs (such as naphthalene, phenanthrene, and tetracene) with weaker transitions (oscillator strength, f, of the type I transition dominating the NUV to NIR spectrum is in the range 10^{-4} to 10^{-3}) tend to correlate with weak, narrow DIBs (normalized equivalent widths $W/E[B-V]$ of the order of 0.01). If verified for a larger set of PAH ions, this observed characteristic would imply similar abundances for catacondensed (noncompact) and pericondensed (compact) PAH ions in the interstellar medium although the latter would contribute more heavily to the visual extinction. In summary, the implications of such a proposal would be that the ~ 50 strong-to-moderate DIBs would be carried by compact PAH ions while the 100 or so weak DIBs which contribute to only 1/5 of the total DIB equivalent width would be associated with noncompact PAH ions and/or with the weaker transitions of compact PAH ions.

That specific PAH structures are far more stable than others and thus dominate the interstellar population is central to the PAH-DIB hypothesis. This is illuminated here by considering the isomer "explosion." To illustrate this point consider the following hypothetical reasoning. Recalling that the typical visible PAH ion spectrum is dominated by one or two bands, the observed 50 DIBs listed in Table 2 would only require 25–50 PAHs, each containing $\sim 0.04\%$–0.02% of the elemental C. The observed interstellar PAH abundance can be fitted by an extrapolation of the MRN interstellar grain-size distribution (Mathis, Rumple, & Nordsieck 1977) into the molecular domain (Tielens 1988). In the resulting mathematical relation, taken from Schutte, Tielens, & Allamandola (1993), the total number of PAHs per interstellar hydrogen atom containing between n_C and $n_C + dn_C$ carbon atoms is given by

$$(dN_{PAH}/N_H) = 1.24 \times 10^{-6} n_C^{-11/6}\, dn_C \quad \text{with} \quad n_C \geq 20 .$$

Adopting this size distribution, PAH abundances (relative to interstellar hydrogen and carbon) and the amounts of cosmic C tied up in PAHs in various molecular size bins can be calculated. These values are summarized in Table 3. Note that the fact that PAHs comprised of 20–100 C atoms seem to consume all the fraction of cosmic C thought to be tied up in PAHs (i.e.,

TABLE 3

PAH Size Distribution

Number of Carbon Atoms (1)	N_{PAH}/N_H (2)	N_{PAH}/N_C (3)	Total Isomer Number[a] (4)	Most Stable Isomer Number[b] (5)	% Cosmic Carbon (6)
20–24	2.2×10^{-8}	5.8×10^{-5}	43	11 [1]	0.13
25–34	2.6×10^{-8}	6.9×10^{-5}	2,501	170 [15]	0.20
35–49	2.0×10^{-8}	5.4×10^{-5}	1,272,650	13,596 [999]	0.22
50–74	1.7×10^{-8}	4.4×10^{-5}			0.27
75–100.....	9.0×10^{-9}	2.4×10^{-5}			0.21

[a] The total isomer number is derived by summing all of the hypothetical isomers calculated by Brunvoll, Cyvin, & Cyvin (1992) for PAHs containing the number of carbon atoms listed in col. (1).

[b] The most stable isomer number is that subset of isomers listed by Brunvoll et al. (1992) with the lowest Dias parameters (1, 0, $-n$ ...). [ ] indicate the number of isomers with negative Dias parameters.

on the order of 1%; see above) does not reflect a serious size constraint. It reflects only the limitations of the size distribution formula (used here only for illustrative purposes). Hence, adopting the total number of different PAHs derived above, we can conclude that each bin must be dominated by ~5–10 abundant interstellar PAHs in order to provide the observed DIB equivalent widths (W_λ's).

This number stands in sharp contrast with the number of possible PAH isomers (different molecular structures with the same number of C and H atoms) in each bin which is also listed in Table 3. Clearly, nature has to be very selective in order for PAHs to be the carriers of the DIBs. This selectivity can be understood in terms of both "practicality" as well as thermodynamic stablity. First, it must be kept in mind that the numbers of isomers reported in Table 3 are calculated using purely mathematical considerations (i.e., without considering any physical and chemical constraints which may forbid the formation of many [if not most] of these structures). The importance of this "weeding out" of unrealistic and/or less stable structures is *pivotal* to the PAH-DIB hypothesis (van der Zwet & Allamandola 1985; Léger & d'Hendecourt 1985; Crawford et al. 1985). To illustrate the dramatic role of thermodynamic stability, consider that of all the PAH structures possible containing about 40 carbon atoms, only nine are fully benzenoid, i.e., each carbon atom in the structure is fully aromatic. These were caled "super aromatics" by Clar (1972). If one uses thermodynamic stability criteria instead of molecular orbital criteria, one finds that there are only six PAH structures which are most stable in building up PAHs containing about 25 carbon atoms (Stein 1978). This is in stark contrast with the large number of isomers possible. Using the criterion of percent resonance energy in adition to thermodynamic stablity has proved insightful in understanding why some PAHs are found in the environment, while others are not (Aihara 1988). The importance of this chemical specificity is often encountered in natural systems. Laboratory experiments show that in hydrocarbon sooting flames, five specific PAHs typically dominate the total abundance of small PAHs (Homann 1979). Theoretical studies show that the condensed PAHs (pyrene, coronene, ovalene, circumcoronene, ...) are the most thermodynamically stable PAHs (Stein 1978), and indeed these are thought to play a key role in soot formation in hydrocarbon flames and in the outflows from C-rich giants (Frenklach & Feigelson 1989; Cherchneff & Barker 1992).

4.2. *Collective Behavior*

The distribution of PAH charge state as a function of PAH size, structure, and properties such as electron affinity described in § 2 can be used to understand the complex collective behavior of the DIBs as a function of the physical conditions along different sight lines. For a specific PAH, when the electron density or UV field changes, variations in the strengths of bands due to its cations and/or anions should anticorrelate with bands due to the same species in neutral form. The same applies when comparing absorptions due to cations as a class with those of anions. Furthermore, the electron affinity, which governs the charge distribution for a given PAH under a specific set of conditions, changes markedly with PAH size and structure. The electron affinity also depends on the nature of any side group present. These properties can produce behavior similar to that observed for the DIBs. For example, while nearly all of the well-known DIBs are moderately strong along the line of sight to σ Sco, a sight line with weak bands due to CH, CH^+, and CN^+; only a few DIBs are strong and many are substantially weaker toward ζ Oph (see, e.g., Snow 1992; Krelowski et al. 1992). While both lines of sight have similar color excesses ($E[B-V] = 0.35$ for σ Sco and 0.33 for ζ Oph], this behavior is generally taken to indicate that the diffuse matter toward σ Sco experiences a far stronger UV field. Hence, within the framework of the PAH-DIB hypothesis, the weaker bands toward σ Sco are likely due to PAH anions or neutrals, while the stronger bands would be due to cations. The oft-quoted statement that the DIBs tend to be weaker relative to the color excess $E(B-V)$ in dense clouds than in the more diffuse interstellar medium (Wampler 1966; Snow and Cohen 1974; Snow 1992; Snow et al. 1995) is entirely consistent with the PAH charge behavior described in § 2 for the smaller members of the PAH family. For such PAHs, the cation fraction decreases with depth in the cloud due to the decrease in the FUV field intensity (see § 2.3 and Fig. 4).

Furthermore, Krelowski and coworkers have shown that there are DIB "families"—groups of bands that seem loosely connected. Certain interstellar conditions favor one family of carriers over the others. This is just the sort of behavior one would expect if a mixture of PAHs were responsible for many of the DIBs. In a general sense, and within the framework of the PAH-DIB hypothesis, we can expect that the DIB carriers can be separated into three distinct families of species: anions, cations, and neutrals. The first have large electron affinities and thus must contain large, planar PAHs of more than about 25 C atoms (or PAHs in the less stable catacondensed [noncompact] form). The second group has small electron affinities and is therefore comprised of small (<25 C atom), compact and noncompact PAHs. Since only neutral PAHs containing more than about 25 C atoms will show absorption bands in the visible (Fig. 8), the third group is comprised of large PAHs. For example, if the spectrum of a PAH in a single charge state comprised several comparably strong bands, they would always correlate tightly. However, the spectrum of many charged PAHs is dominated by a single strong transition in the spectral region of interest (see § 3). Thus, while bands arising from PAHs with similar properties (such as size and electron affinity) would tend to go together, they would not be as tightly coupled as the bands from one single PAH in one charge state. Collectively, these bands would behave very differently from those arising from PAHs with different properties. Thus, *within the framework of the PAH hypothesis, DIB families could provide tracers of conditions within a cloud which*

TABLE 4

POTENTIAL CONTRIBUTION OF PAHS TO THE DIBS AS A FUNCTION OF MOLECULAR SIZE, STRUCTURE, AND CHARGE STATE

Number of C Atoms	Structure	Charge State	Contribution to the DIBs
$N_C < 25$	Compact	+	Yes
		0	No
	Noncompact	+	Yes
		−	Yes
		0	No
$25 \leq N_C \leq 250$	Planar	−	Yes
		0	Yes
$250 < N_C < 1000$.....	Planar	−	No
		0	Yes
$N_C \geq 1000$ up to ..... graphitic limit	Spherical	+	No
		0	Yes

globally determine the relative importance of cations, anions, and neutral species, rather than tracers of a specific species.

5. CONCLUSIONS

An assessment of the PAH-DIB proposal is presented based on the detailed consideration of the physical properties (charge distribution and related spectral signatures) of PAHs expected in the diffuse interstellar medium. The conditions to be met by the PAHs (as well as by any other molecular candidates) as potential DIB carriers can be stated as follows (Snow 1995):

1. Stability under interstellar conditions;
2. Compatibility with cosmic abundances;
3. Consistency with the environment;
4. Relevance of spectral features;
5. Internal consistency (i.e., family of molecules with appropriate physical properties).

The focus here has been on how to further constrain and test the PAH-DIB proposal. The main conclusions of the study are outlined in Table 4 and can be stated as follows.

1. *The diffuse ISM environment produces a mixture of neutral as well as positively and negatively charged PAHs.* The relative proportions of each depend on the physical conditions (density, UV field) in the cloud(s) along the line of sight, as well as on the specific properties (ionization potential and electron affinity) of the particular PAHs under consideration. Each PAH has a distinct spectral signature depending on its charge state (-1 [anion], 0 [neutral], and $+1$ [cation]).

It is found that small compact PAHs (less than 25 carbon atoms) will be distributed between cations and neutrals while their noncompact counterparts will be equally distributed between cations, anions, and neutrals. Larger planar species ($N_C = 100$) will be distributed between anions and neutrals. Finally, grain-type structures ($N_C = 10^3$) will be distributed between cations and neutrals. Moreover, the charge distribution is expected to vary as a function of depth within a single cloud, shifting toward more negatively charged species with increasing depth.

2. *The change in the distribution of PAH charge states as a function of PAH size and structure can account for the complex collective behavior of the DIBs as a function of the physical conditions along different lines of sight.* When the electron density or UV field changes, variations in the strengths of bands due to ionized PAHs should anticorrelate with bands due to the same PAHs in neutral form.

Thus, bands arising from PAHs with similar properties (such as size and electron affinity) would tend to go together, although they would not be as tightly coupled as the bands from one specific PAH in one particular charge state. Collectively, these bands would behave very differently from those arising from PAHs with different properties. *The direct implication is that the DIB carriers can be separated into three distinct families of species: anions, cations, and neutrals and that within the framework of the PAH hypothesis, DIB families are tracers of conditions within a cloud which globally determine the relative importance of cations, anions, and neutral species, rather than tracers of a specific species.*

3. A small fraction of the cosmic carbon is required to be in the form of PAHs to account for the total equivalent width of all the DIBs combined. *A limited number of PAHs must dominate, however, the interstellar PAH distribution in order to provide the finite number of DIBs observed.* This type of chemical specificity, often encountered in natural systems, is a critical constraint for the PAH-DIB proposal.

Thus, while all neutral PAH molecules containing more than about 30 carbon atoms absorb in the visible and NIR ranges and are potential candidates for the DIBs, the large increase in the number of stable isomers with increasing size limits the potential importance of large PAHs as DIB carriers. In contrast, in the case of singly ionized PAHs (cations and anions), only the smaller molecular ions (less than about 250 carbon atoms) can potentially contribute to the DIBs. *Since the DIBs are expected/postulated to be carried by a finite number of molecular species belonging (mostly) to the same chemical family and present under different charge states, it is tempting to correlate the known DIBs with the 150–200 stable PAH ions belonging to the class of smaller PAHs.*

4. *Since PAH ion spectra are dominated by a single band in the DIB spectral range,* it seems reasonable to assume that the PAH-DIB correlation can be made on the basis of "one PAH-one DIB" (i.e., each individual PAH produces one DIB). Moreover, the observed distribution of the DIBs between strong/moderate and broad bands on the one hand and weak and narrow bands on the other hand can also be interpreted in the context of the PAH proposal. Thus, it is found that *compact PAH ions which have a spectrum dominated by a strong (type A) transition correlate with strong and broad DIBs while noncompact PAHs, which have a spectrum dominated by a weaker (type I) transition, correlate with weak and narrow DIBs.*

In conclusion, the PAH-DIB proposal seems extremely promising. This proposal requires that the interstellar PAH distribution is dominated by a small, finite number of species (100–200). A further test of the PAH proposal requires detailed laboratory studies in the far and vacuum ultraviolet regions of the absorption properties of neutral and ionized PAHs and an observational search for bands in these regions.

This work has been supported by NASA Astrophysics Division under the following programs: Ultraviolet and Visible Astrophysics (grant 188-41-57-41), Infrared and Radio Astrophysics (grant 188-414-57-01), Long-Term Space Astrophysics (grant 399-20-00-05), and Astrophysics Theory (grants NAG5-2858 and 399-20-10-13).

APPENDIX

Before discussing the spectroscopic properties of PAHs, we briefly review the basic nomenclature practices adopted for this family of molecules (Jaffé & Orchin 1962, Chap. 13 and references therein; Gutman & Cyvin 1989).

The prototype PAHs consist solely of fused six-membered benzenoid rings of sp^2-hybridized carbon atoms and the requisite number of hydrogen atoms attached to the periphery of the molecule (some representative PAHs are shown in Fig. 1). Hence, neutral benzenoid PAHs are assumed to be *planar*. However, there is evidence for nonplanar structures beyond a certain size and for geometries that produce intramolecular steric strain: hydrogen-hydrogen interference and/or the presence of overlapping rings

(Fetzer 1989; Herndon 1990). The carbon skeletons, also called polyhex systems (Gutman & Cyvin 1989), can be grouped into two large classes:

1. Pericondensed aromatics where some carbon atoms belong to three rings (pyrene, perylene, benzo(g, h, i)perylene, ...). This class also includes molecules of empirical formula ($C_{6n^2}H_{6n}$ that represent *the most stable structures* for a given number of rings and are often referred to as "superaromatic" (e.g., coronene and circumcoronene; Clar 1972).
2. Catacondensed aromatics of empirical formula $C_{4n+2}H_{2n+4}$ where no carbon atom belongs to more than two rings. Three subclasses can be further defined in this case. The acenes are systems in which all the rings are joined linearly such as anthracene, tetracene, pentacene, ... The phenes contain an angular or bent system of rings such as phenanthrene, tetraphene, pentaphene, ... A third case regroups PAHs that belong to neither the acenes nor the phenes (such as chrysene, benzo(c)phenanthrene, picene, ...).

Catacondensed PAHs are generally expected to be less stable than pericondensed PAHs with the same number of rings due to differences inherent in the resonance energy of each type.[8]

A.1. NEUTRAL PAHS

The spectroscopic properties of neutral PAHs have been extensively documented thanks to the pioneering work of Clar (1964) and Platt (1949). In the visible and near-infrared ranges, the spectroscopy of PAHs is described by vibronic transitions occurring within the π electron system of the molecules (Fig. 7). The π electron system is comprised of the bonding (π) and antibonding (π^*) orbitals. Neutral PAHs are closed-shell molecules, i.e., their bonding levels are completely filled and the antibonding levels are empty. These two sets of levels are separated by an energy gap whose size decreases with increasing number of carbon atoms in the molecule. The separation between the peaks in the π and π^* electron level distribution function, however, remains constant at about 5 eV (Robertson 1986). This implies that the strongest transition will occur around 5 eV—the separation between the peaks in the electron energy distribution function. This first-order approximation is reasonably well verified in the case of large PAHs (i.e., 100 carbon atom PAHs up to the graphitic limit) where a macroscopic description of the system is valid. This is not the case for the smaller PAHs, however, where a molecular description is more appropriate. In this latter case, symmetry arguments, which can no longer be ignored, and the derived spectroscopic selection rules dictate the strength of each of the individual transitions (e.g., the compact PAHs hexabenzocoronene [$C_{42}H_{18}$], circobiphenyl [$C_{38}H_{16}$], ovalene [$C_{32}H_{14}$], and coronene [$C_{24}H_{12}$] have their strongest transition at 3.4, 3.3, 3.6, and 4.1 eV, respectively [Dias 1987, pp. 326, 370, 383, 388]). The absorption spectra of some representative small PAHs are shown in Figure 6 to illustrate this point.

The transitions correspond to the excitation of a π electron from one of the HOMOs of the π system to one of the LUMOs of the π^* system (Fig. 7*a*). The transitions, expressed as linear combinations of the electron configurations associated with the molecular orbital electron occupancies, give rise to bands which have traditionally been classified as α, para (p), β, and β' following Clar's notation (Clar 1964) or $L_{a,b}$ and $B_{a,b}$ following Platt's notation (Platt 1949).[9] The α band system is characterized by a very weak oscillator strength (f of the order of 0.001). It is the first band system (i.e., lowest energy) in approximately one-half of all PAHs studied. The p band system is the intermediate-wavelength absorption and is weak with an oscillator strength, f, of the order of 0.01–0.1. This transition occurs as either the first or second band system in the spectra. The p bands are generally more sensitive to variations in structure than the α bands and this results in the α bands being overtaken by the p bands as the molecular size increases. The β band system occurs at shorter wavelengths and is the strongest absorption with an oscillator strength, f, of the order of 1. Clar (1972) has noted that the spectra of many PAHs follow the empirical relationship $\lambda_\alpha/\lambda_\beta \cong 1.35$. Finally, the shortest wavelength band system, β', has an oscillator strength, f, intermediate between that of the β and p band systems. These notations are, however, used only for convenience as a label of the absorption spectra since they do not provide information on the exact symmetry of the specific electronic states involved in the transitions observed. Moreover, although the relative intensity ratios of the different band systems hold reasonably well for catacondensed PAHs, this is not the case for some pericondensed PAHs (i.e., pyrene, coronene, ovalene) where the oscillator strengths of the band systems can be, in some cases, of the same order of magnitude.The band systems are generally well separated through polarization studies which show that the α and β systems are longitudinally polarized while the p and β' systems are transversely polarized with respect to the long axis of the molecule.

Exhaustive studies of the absorption spectra of the smaller neutral PAHs (comprised of up to about six benzene rings) have shown that the strongest absorptions lie in the UV and NUV range (e.g., Jaffé & Orchin 1962; Birks 1970). These studies have also shown that the three band systems shift to longer wavelengths when the number of benzenoid rings increases. This effect, called the annellation effect, is particularly true for the catacondensed PAHs but does suffer some exceptions in the case of the pericondensed species (Clar 1964, 1972). An empirical formula ($\lambda = K^2/R$) has been derived, in the case of the catacondensed PAHs, to calculate the longest wavelength component of each absorption band system. In the formula, K is the order number and is a function of the number of π electrons in the molecule while R is a constant characteristic of the α, β, and p bands (Jaffé & Orchin 1962). In a similar attempt for pericondensed PAHs, Schutte et al. (1993) have recently derived a linear relationship between the cut-off wavelength of the strongest absorption system (β) and the average size of the molecule.

A.2. PAH IONS

Contrary to the neutral precursors which are closed shell species (i.e., all of the low-lying molecular orbitals are filled with paired electrons), cations and anions are open-shell species. The unpaired electron is, however, considerably delocalized and radical ions of

[8] The resonance energy per π electron (REPE) of a PAH is defined as the difference between the calculated Hückel molecular orbital (HMO) π energy and the π energy of an equivalent structure where the π bonds are localized, divided by the number of π electrons. This quantity is shown to correlate well with experimental stability (Hess & Schaad 1970; Aihara 1977).

[9] Note.—For gas-phase molecules, each absorption band system includes transitions between the individual rotational and vibrational levels associated with each of the two electronic states involved in the transition. These transitions are called *rovibronic* to express their rotational, vibrational, and electronic characters.

TABLE 5

ONE-ELECTRON TRANSITIONS WITHIN THE π LEVELS OF PAH IONS

Type	Cation	Anion
I	$n - i \rightarrow n;\ 1 \leq i \leq n-1$	$n+1 \rightarrow n+i;\ 2 \leq i \leq n$
A.....	$n \rightarrow n+1$	$n \rightarrow n+1$
B.....	$n - i(1 \leq i \leq n-1) \rightarrow n + i(1 \leq i \leq n)$	$n - i(1 \leq i \leq n-1) \rightarrow n + i(1 \leq i \leq n)$
	$n \rightarrow n+i;\ 2 \leq i \leq n$	$n \rightarrow n+i;\ 2 \leq i \leq n$

NOTE.—1 to n represent bonding and $(n+1)$ up to $2n$ are antibonding states.

PAHs are also considered to be π-type molecular ions (e.g., Werst & Trifunac 1991). Besides the $\pi \rightarrow \pi^*$ transitions which are similar to those possible in neutral PAHs, transitions within the π (cations) or the π^* (anions) levels now also become possible (Fig. 7). The one-electron transitions occurring within the π levels of either the cations and anions can be classified according to the three types shown in Table 5 (Shida & Iwata 1973; Khan 1984).

In the case of the cations, all transitions of type I occur within the HOMO manifold and correspond to transitions from doubly occupied π orbitals (π^2) to a single occupied π orbital (π^1). In the case of the anions, all transitions of type I are within the LUMO manifold and correspond to transitions from a single occupied π (π^1) to a nonoccupied π (π^0). Type I transitions have, thus, no analogs in the neutral. In contrast, an analogy can be drawn between the type A transition in the ions and the neutral's p transition and between the type B transitions of the ions and the (α, β) transitions in the neutral (compare Figs. 7*b* and 7*c* with Fig. 7*a*). To first order, the π and π^* levels of a PAH molecule are mirror images and, hence, the longest wavelength transitions of the cation and anion of a particular PAH occur at very similar wavelengths (see Figs. 7*b* and 7*c*). The energy level separation is of the order of 6 eV/N_C and, hence, even the smallest PAH ion (naphthalene $C_{10}H_8^+$ and/or $C_{10}H_8^-$) will have transitions in the visible.[10]

Few experimental data are available on the spectroscopy of charged PAHs. In addition to the pioneering work of Hoijtink and his colleagues (Hoijtink 1959; Hoijtink & Zandstra 1960), the most exhaustive information on the absorption spectroscopy of PAH ions comes from the works of Shida & Iwata (1973), Shida (1988), Khan (1984, 1987, 1988, 1991, 1992) and, very recently, Lee & Wdowiak (1993). In all cases, monocation and monoanion PAHs were formed by photolysis or radiolysis of the neutral precursor trapped in organic matrices and glasses. The advantage of this technique is to provide a straightforward way to isolate the molecular ions in the solid at temperatures ranging from 77 K to room temperature and to study their general properties. The principal disadvantage, from the astrophysical point of view, comes from the strong perturbations induced by the matrix environment on the energy levels of the trapped molecular ions. This interaction between the PAH ion and its environment results in large shifts of the electronic transitions compared to the "ideal" case of a free, isolated PAH ion. Recently, however, an effort has been made to measure the spectroscopic properties of minimally perturbed PAH cations by studying the spectroscopy of PAHs in media astrophysically relevant, i.e., PAHs truly isolated at low temperature (4–10 K) in an inert medium (ideally in a neon matrix: Salama & Allamandola 1991a, b, 1992a, b, 1993; Salama et al. 1994, 1995; Ehrenfreund et al. 1992 a, b, 1995; Léger et al. 1995 also, to a lesser extent, in the more polarizable argon matrix: Andrews, Kelsall, & Blankenship 1982; Andrews, Friedman, & Kelsall 1985; Kelsall & Andrews 1982, Szczepanski et al. 1992, 1993; Vala et al. 1994). Photoelectron spectroscopy (PES) studies of an extensive set of PAHs also provide information on some of the electronic states of the monocations in the gas phase (Boschi & Schmidt 1972; Clark, Brogli & Heilbronner 1972; Boschi, Clar & Schmidt 1974; Clar & Schmidt 1976; Schmidt 1977). This limitation in the analogy between optical and photoelectron spectra is due to the fact that the correlation between optical spectroscopy and PES is valid only for type I transitions, i.e., $\pi^2 \rightarrow \pi^1$ transitions (see Fig. 7*b*). Until molecular jet spectroscopy and/or ion trapping techniques are developed and adapted to study cold, isolated PAH ions in the gas phase, neon-matrix isolation spectroscopy (MIS) remains the best tool available to laboratory astrophysicists to simulate the conditions of the diffuse interstellar medium. Finally, the availability of MIS data has stimulated new, semiempirical, quantum chemical calculations (Parisel, Berthier, & Ellinger 1992; Du et al. 1993; Negri & Zgierski 1994; Parisel & Ellinger 1994). Although the recent calculations predict the energetic position of the electronic states of PAH cations with an improved accuracy, the calculated oscillator strengths show (in the case of catacondensed PAHs) a very large discrepancy with the experimentally measured oscillator strengths.

[10] It is important to stress, here again, that the electronic transitions of gas-phase ions also involve the vibrational and rotational levels of the initial (ground) and final (excited) electronic states. Moreover, the two electronic states have different electron configurations and, hence, different rotational and vibrational constants. This has two important implications in the context of the DIB discussion. First, the (ro)vibronic transitions must be considered in any experimental or theoretical study of DIB candidates (PAHs in our case). Second, it must be recognized that one *does not expect to observe exactly the same* vibrational spacings in the diffuse interstellar absorption bands and the IR emission bands. The IR emission bands originate from the ground electronic state whereas the DIB spacing would be associated with the upper electronic state and there could be small differences.

REFERENCES

Abouelaziz, H., Gomet, J. C., Pasquerault, D., & Rowe, B. R. 1993, J. Chem. Phys., 99, 237
Adamson, A. J., Whittet, D. C. B., & Duley, W. W. 1991, MNRAS, 252, 234
Aihara, J. 1977, J. Am. Chem. Soc., 99, 2048
———. 1988, Bull. Chem. Soc. Japan, 61, 1451
Allamandola, L. J., Tielens, A. G. G. M., & Barker, J. R. 1985, ApJ, 290, L25
———. 1989, ApJS, 71, 733
Andrews, L., Friedman, R. S., & Kelsall, B. J. 1985, J. Phys. Chem., 89, 4016
Andrews, L., Kelsall, B. J., & Blankenship, T. A. 1982, J. Phys. Chem., 86, 2916
Bakes, E. L. O., & Tielens, A. G. G. M. 1994, ApJ, 427, 822
Birks, J. B. 1970, in Photophysics of Aromatic Molecules, ed. J. Birks (London: Wiley) 70
Boschi, R., Clar, E., & Schmidt, W. 1974, J. Chem. Phys., 60, 4406
Boschi, R., & Schmidt, W. 1972, Tetrahedron Lett., 25, 2577
Brunvoll, J., Cyvin, B. N., & Cyvin, S. J. 1992, in Advances in the Theory of Benzenoid Hydrocarbons II, ed. I. Gutman (Heidelberg: Springer), 181
Burtscher, H. 1992, J. Aerosol Sci., 23, 549
Cherchneff, I., & Barker, J. R. 1992, ApJ, 394, 703
Clar, E. 1964, Polycylic Hydrocarbons (New York: Academic Press)
———. 1972, The Aromatic Sextet (London: Wiley)

Clar, E., & Schmidt, W. 1976, Tetrahedron, 32, 2563
Clark, P. A., Brogli, F., & Heilbronner, E. 1972, Helvetica Chim. Acta, 55, 1415
Cohen, M., & Jones, B. F. 1987, ApJ, 321, L151
Crawford, M. K., Tielens, A. G. G. M., & Allamandola, L. J. 1985, ApJ, 293, L45
Dias, J. R. 1987, in Handbook of Polycyclic Hydrocarbons, Part A (Amsterdam: Elsevier)
Draine, B. T., & Sutin, B. 1987, ApJ, 320, 803
Du, P., Salama, F., & Loew, G. H. 1993, Chem. Phys., 173, 421
Ehrenfreund, P., d'Hendecourt, L., Joblin, C., & Léger, A. 1992b, A&A, 266, 429
Ehrenfreund, P., d'Hendecourt, L., Verstraete, L., Léger, A., Schmidt, W., & Défourneau, D. 1992a, A&A, 259, 257
Ehrenfreund, P., Foing, B. H., d'Hendecourt, L., Jenniskens, P., & Désert, X. 1995, A&A, 299, 213
Fetzer, J. C. 1989, in Chemical Analysis of Polycyclic Aromatic Compounds, ed. T. Vo-Dinh (London: Wiley), 59
Fossey, S. F. 1990, Ph.D. Thesis, Univ. London
———. 1991, Nature, 353, 393
Frenklach, M., & Feigelson, E. D. 1989, ApJ, 341, 372
Gallegos, E. J. 1968, J. Phys. Chem., 72, 3452
Gutman, I., & Cyvin, S. J. 1989, in Introduction to the Theory of Benzenoid Hydrocarbons, ed. I. Gutman & S. J. Cyvin (Heidelberg: Springer), 13
Habing, H. J. 1968, Bull. Astron. Inst. Netherlands, 19, 421
Heger, M. L. 1922, Lick Obs. Bull., Vol. 10, No. 337, 146
Herbig, G. H. 1975, ApJ, 196, 129
———. 1988, ApJ, 331, 999
———. 1993, ApJ, 407, 142
Herbig, G. H., & Leka, K. D. 1991, ApJ, 382, 193
Herndon, W. 1990, J. Am. Chem. Soc., 112, 4546
Hess, B. A., & Schaad, L. J. 1970, J. Am. Chem. Soc., 93, 2413
Hoijtink, G. J. 1959, Molec. Phys., 2, 85
Hoijtink, G. J., & Zandstra, P. J. 1960, Molec. Phys., 3, 371
Homann, K. H. 1979, Ber. Bunsenges. Phys. Chem., 83, 738
Jaffé, H., & Orchin, M. 1962, in Theory and Applications of Ultraviolet Spectroscopy, (London: Wiley)
Jenniskens, P., & Désert, X. 1994, A&AS, 106, 39
Joblin, C., Maillard, J. P., d'Hendecourt, L. B., & Léger, A. 1990, Nature, 346, 729
Kelsall, B. J., & Andrews, L. 1982, J. Chem. Phys., 76, 5005
Khan, Z. H. 1984, Z. Nat., 39a, 668
———. 1987, Z. Nat., 42a, 91
———. 1988, Spectrochim. Acta, 44A, 313
———. 1991, Canadian J. Appl. Spectrosc., 37, 82
———. 1992, Acta Phys. Pol., A82, 937
Khan, Z. H., Husain, M. M., & Haselbach, E. 1993, Appl. Spectrosc., 47, 2140
Khan, Z. H., & Schmidt, W. 1985, in Proc. 3rd Conference on Lasers, Atomic, and Molecular Physics (reprint)
Krewlowski, J., & Sneden, C. 1993, PASP, 105, 1141
———. 1994, in The First Symposium on the Infrared Cirrus and Diffuse Interstellar Clouds, ed. R. Cutri & W. Latter (ASP Conf. Ser., 58), 12
Krelowski, J., Snow, T. P., Papaj, J., Seab, C. G. B., & Wszolek, J. 1993, ApJ, 419, 692
Krelowski, J., Snow, T. P., Seab, C. G. B., & Papaj J. 1992, MNRAS, 258, 693
Krelowski, J., & Walker, G. A. H. 1987, ApJ, 312, 860
Leach, S. 1987, in Polycylic Aromatic Hydrocarbons and Astrophysics, ed. A. Léger et al. (Dordrecht: Kluwer) p. 99
———. 1989, in Interstellar Dust, ed. L. Allamandola & A. Tielens (Dordrecht: Kluwer) p. 155
Le Bertre, T. 1990, A&A, 236, 472
Le Bertre, T., & Lequeux, J. 1993, A&A, 274, 909
Lee, W., & Wdowiak, T. J. 1993, ApJ, 410, L127
Léger, A., & d'Hendecourt, L. B. 1985, A&A, 146, 81
Léger, A., d'Hendecourt, L. B., & Défourneau, D. 1995, A&A, 293, L53
Mathis, J. S., Rumple, W., & Nordsieck, K. H. 1977, ApJ, 217, 425
Merrill, P. W. 1934, PASP, 46, 206
Negri, F., & Zgierski, M. Z. 1994, J. Chem. Phys., 100, 1387
Parisel, O., Berthier, G., & Ellinger, Y. 1992, A&A, 266, L1
Parisel, O., & Ellinger, Y. 1994, in The Diffuse Interstellar Bands: Contributed Papers, ed. A. Tielens (NASA Conf. Pub. 10144), 91
Platt, J. R. 1949, J. Chem. Phys., 17, 484
Pritchet, C. J., & Grillmair, C. J. 1984, PASP, 96, 349
Rao, N. K., & Lambert, D. L. 1993, MNRAS, 263, L27
Robertson, J. 1986, Adv. Phys., 35, 317
Salama, F. 1993, J. Chem. Soc. Faraday Trans., 89, 2308
Salama, F., & Allamandola, L. J. 1991a, J. Chem. Phys. 94, 6964
———. 1991b, J. Chem. Phys., 95, 6190
———. 1992a, ApJ, 395, 301
———. 1992b, Nature, 358, 42
———. 1993, J. Chem. Soc. Faraday Trans., 89, 2277
Salama, F., Joblin, C., & Allamandola, L. J. 1994, J. Chem. Phys., 101, 10252.
———. 1995, in The Diffuse Interstellar Bands, ed. A. Tielens & T. Snow (Dordrecht: Kluwer) 207
Sanner, F., Snell, R., & Vanden Bout, P. 1978, ApJ, 226, 460
Sarre, P. J. 1991, Nature, 351, 356
Scarrott, S., Watkin, S., Miles, J. R., & Sarre, P. J. 1992, MNRAS, 255, 11P
Schmidt, W. 1977, J. Chem. Phys., 66, 828
Schutte, W., Tielens, A. G. G. M., & Allamandola, L. J. 1993, ApJ, 415, 397
Shida, T. 1988, in Electronic Absorption Spectra of Radical Ions, ed. T. Shida (Amsterdam: Elsevier)
Shida, T., & Iwata, S. 1973, J. Am. Chem. Soc., 95, 3473
Smith, F. T. 1961, J. Chem. Phys., 34, 793
Snow, T. P. 1992, Australian J. Phys., 45, 543
———. 1995, in The Diffuse Interstellar Bands, ed. A. Tielens & T. Snow (Dordrecht: Kluwer) 379
Snow, T. P., & Cohen, J. G. 1974, ApJ, 194, 313
Snow, T. P., Krelowski, J., Seab, C. G., Wszolek, B., & Papaj, J. 1995, in preparation
Snow, T. P., & Seab, C. G. 1991, ApJ, 382, 189
Somerville, W. B. 1993, J. Chem. Soc. Fraday Trans., 89, 2308
Spitzer, L. 1978, in Physical Processes in the Interstellar Medium (New York: Wiley), 52
Stein, S. E. 1978, J. Phys. Chem., 82, 566
Stein, S. E., & Brown, R. L., 1991, J. Am. Chem. Soc., 113, 787
Streitwieser, A. 1961, in Molecular Orbital Theory for Organic Chemists (New York: Wiley)
Szczepanski, J., Roser, D., Personette, W., Eyring, M., Pellow, R., & Vala, M. 1992, J. Phys. Chem., 96, 7876
Szczepanski, J., Vala, M., Talbi, D., Parisel, O., & Ellinger, Y. 1993, J. Chem. Phys., 98, 4494
Tielens, A. G. G. M. 1988, in Submillimeter and Millimeter Astronomy, G. Watt & A. Webster (Dordrecht: Kluwer) 13
Tobita, S., Meinke, M., Illenberger, E., Christophorou, L. G., Baumgartel, H., & Leach, S. 1992, Chem. Phys., 161, 501
Tripp, T. M., Cardelli, J. A., & Savage, B. D. 1994, AJ, 107, 645
Vala, M., Szczepanski, J., Pauzat, F., Parisel, O., Talbi, D., & Ellinger, Y. 1994, J. Phys. Chem., 98, 9187
Van der Zwet, G. P., & Allamandola, L. J. 1985, A&A, 146, 76
Van Dishoeck, E. F., & Black, J. H. 1986, ApJS, 62, 109
Verstraete, L., Léger, A., d'Hendecourt, L., Dutuit, O., & Défourneau, D. 1990, A&A, 237, 436
Wampler, E. J. 1966, ApJ, 144, 921
Werst, D. W., & Trifunac, A. D. 1991, J. Phys. Chem., 95, 3466